Topological phase transition induced by gain and loss in a photonic Chern insulator

Hau Tian Teo [1], Haoran Xue [1,*] and Baile Zhang [1,2,†]

[1] *Division of Physics and Applied Physics, School of Physical and Mathematical Sciences, Nanyang Technological University, Singapore 637371, Singapore*

[2] *Centre for Disruptive Photonic Technologies, Nanyang Technological University, Singapore 637371, Singapore*

(Received 27 February 2022; accepted 28 April 2022; published 12 May 2022)

We present a design of a non-Hermitian photonic Chern insulator whose band topology can be tuned via gain and loss. It is found that, by continuously varying the gain and loss parameter, a topological phase transition can take place in the photonic crystal, accompanied by the closing and reopening of a Dirac cone. We demonstrate this phenomenon through numerical simulations of the bulk and the edge dispersions, and steady field distributions excited by a point source. Our results show the possibility of non-Hermitian control over band topology in a Chern insulator setting and may find applications in active topological photonic devices.

DOI: 10.1103/PhysRevA.105.053510

Inspired by the discovery of topological materials in condensed-matter systems [1,2], studies on photonic topological phases have grown rapidly in the past decade [3–5]. Starting from the implementation of photonic Chern insulators in gyromagnetic photonic crystals [6,7], various topological phases have been realized in photonic systems, such as analogs of quantum spin Hall insulators [8–12], valley photonic crystals [13–17], photonic Floquet topological insulators [18–21], and photonic Weyl crystals [22–24].

Apart from the developments in constructing various classic topological phases, considerable effort has also been devoted to studying the effects of non-Hermiticity on band topology in photonic systems [25–30], where non-Hermiticity can naturally arise due to gain and/or loss. There are mainly two reasons that motivate the studies on non-Hermitian topological photonic systems. First, non-Hermiticity fundamentally enriches band topology, leading to intriguing physics such as new topological classifications [31,32] and point-gap topology [33]. Various branches of new topological physics can be explored in the context of photonics. Secondly, introducing non-Hermiticity to topological photonics has the potential to lead to useful applications, including the recently invented topological lasers [34].

While most earlier efforts focused on the interplay between non-Hermiticity and topological boundary modes [25,27], many recent studies investigated how non-Hermiticity can drive a topological phase transition in photonic systems [30,35–39]. In point-gapped systems, a topological phase transition can easily happen by simply tuning the non-Hermitian parameters such as anisotropy in the hoppings [30,39]. In line-gapped systems, studies have also shown that it is possible to achieve topological phase transitions that are solely driven by non-Hermitian parameters [35–38,40–42]. Such a non-Hermitian steering of topological phases is promising for active and reconfigurable topological photonic devices. However, most studies on non-Hermiticity-induced topological phase transition in line-gapped systems are based on obstructed atomic insulators [35–37]. Only a few examples of non-Hermiticity-induced topological phase transition between Chern insulators and trivial insulators have been proposed. These examples are all based on tight-binding models [40–42] or ideal transfer matrix models [38], while a realistic photonic model for such a transition is still lacking.

In this work, we report a topological phase transition driven by gain and loss in a non-Hermitian gyromagnetic photonic crystal. Our design is based on a photonic honeycomb lattice comprised of gyromagnetic rods with gain and loss. Through finite-element simulations, we found that the continuously varying gain and loss parameter can lead to the closing and the reopening of the bulk Dirac cone, associated with a topological phase switching between a Chern insulator phase with chiral edge modes and a trivial gapped phase. Such a topological phase transition process is verified numerically by simulations of both edge dispersions and field distributions under a point source excitation at the edge. The proposed phenomenon is ready to be tested in the microwave regime.

As illustrated in Fig. 1, we consider a two-dimensional photonic crystal consisting of gyromagnetic rods arranged in a honeycomb lattice. Under a static external magnetic field in the out-of-plane direction, the relative permeability of the rods is assumed to take the tensor form as follows:

$$\boldsymbol{\mu} = \begin{bmatrix} 0.95 & 0.93i & 0 \\ -0.93i & 0.95 & 0 \\ 0 & 0 & 1 \end{bmatrix}. \tag{1}$$

In addition, the relative permittivities of the red and the blue rods are set to be $\epsilon_+ = 15 + i\gamma$ and $\epsilon_- = 15 - i\gamma$, respectively, where the parameter γ hereby controls the gain and loss in each rod. The rods have diameters of either d_1 or d_2, as shown in Fig. 1. Throughout this work, we fix their values to be $d_1 = 0.462a$ and $d_2 = 0.338a$, respectively, where $a = 17.5$ mm. The unit cell is denoted by the dashed

*haoran001@e.ntu.edu.sg
†blzhang@ntu.edu.sg

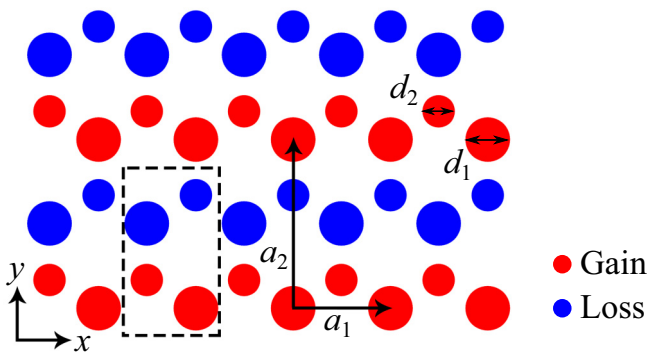

FIG. 1. Design of the 2D non-Hermitian photonic crystal with on-site gain and loss. The red and blue rods are made of gyromagnetic materials with relative permittivity $\epsilon_+ = 15 + i\gamma$ and $\epsilon_- = 15 - i\gamma$, respectively. Here, γ is a positive real number that controls the gain and loss in each rod. The dashed rectangle denotes the unit cell, whereas $\boldsymbol{a_1} = [a,\ 0]$ and $\boldsymbol{a_2} = [0,\ a\sqrt{3}]$ are the lattice vectors. The remaining parameters are the lattice constant $a = 17.5$ mm and the diameters of the rods $d_1 = 0.462a$ and $d_2 = 0.338a$.

rectangle in Fig. 1, with the lattice vectors being $\boldsymbol{a_1} = [a,\ 0]$ and $\boldsymbol{a_2} = [0,\ a\sqrt{3}]$. We note that such a lattice configuration is similar to a recently proposed non-Hermitian Haldane model that exhibits topological phase transition driven by gain and loss [42]. In the following, we study the line-gap topology of the transverse magnetic bands of this photonic crystal through finite-element simulations in the commercial software Comsol Multiphysics.

In the absence of gain and loss, i.e., $\gamma = 0$, the above photonic crystal consisting of gyromagnetic rods is known to exhibit the photonic Chern insulator phase [6,7]. Under the present parameters of the system, a nontrivial band gap with gap Chern number -1 is found between the second and the third bands around 4.68 GHz [see Fig. 2(a)]. Note that, in the non-Hermitian regime, the Chern number can still be defined via a biorthogonal basis [43,44]. Since both time-reversal symmetry and inversion symmetry are broken (due to the external magnetic field and the unequal diameters of the rods, respectively), an unpaired massive Dirac cone is observed [see Fig. 2(e) for the bulk dispersion around the Dirac cone]. In the Hermitian case, the topological phase is determined by the relative strength between the time-reversal symmetry breaking and the inversion symmetry breaking. Thus a topological phase transition can be driven by tuning the external magnetic field or the diameters of the rods. During the transition, the unpaired massive Dirac cone will first close and then reopen. Similar topological phase transitions are commonly found in the systems with competition between time-reversal symmetry breaking and inversion symmetry breaking [45–48]. In the following, we show that the non-Hermitian parameter γ can also drive a topological phase transition besides the Hermitian parameters.

Figures 2(a)–2(d) show the calculated bulk band diagrams along the $k_y = 0$ line with increasing value of the gain and loss parameter γ. As can be seen, the bulk band gap first closes and then reopens as γ increases from 0 to 3.9 (see

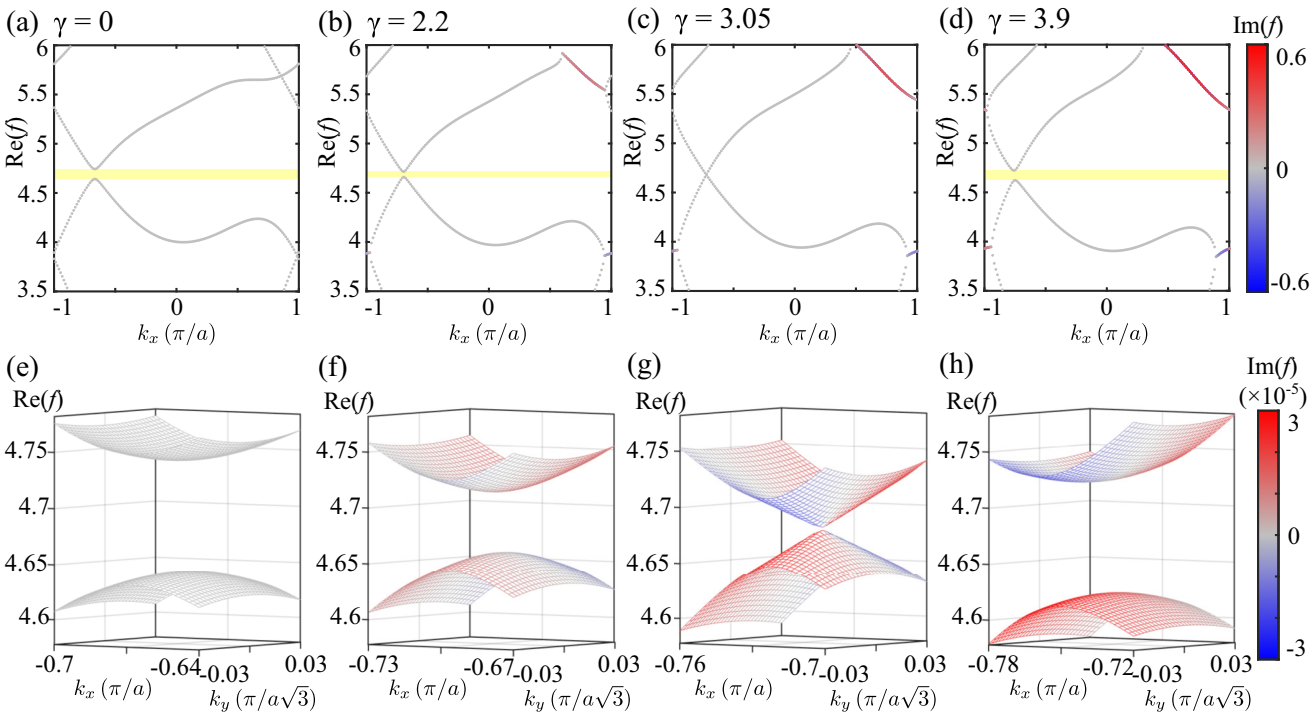

FIG. 2. Plots of bulk band diagrams against the non-Hermitian parameter γ. The first row [panels (a) to (d)] shows the bulk band structures of different γ at $k_y = 0$ with band gaps shaded in yellow. From (a) to (d), the sizes of the band gap are 0.1 GHz, 0.06 GHz, 0 GHz, and 0.1 GHz. The second row [panels (e) to (h)] shows the corresponding bulk band structures near the Dirac cone, where the band gap closes at $\gamma = 3.05$. The eigenfrequencies f are in units of GHz and the color scale in each panel indicates the imaginary part of the eigenfrequencies.

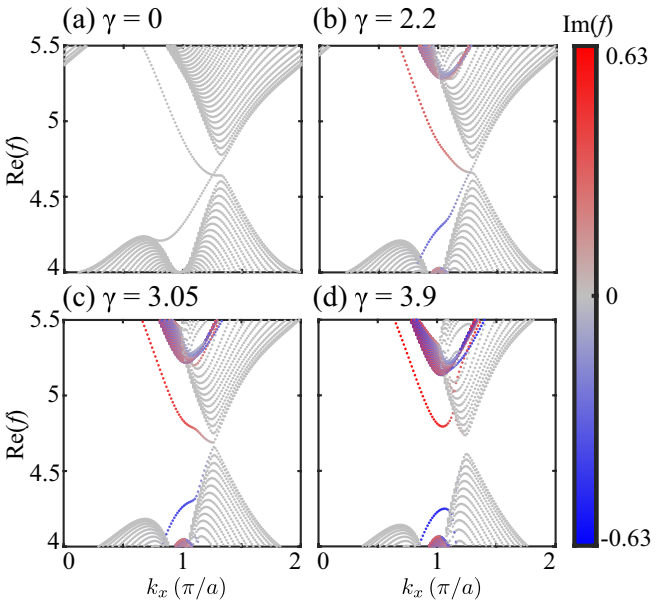

FIG. 3. Plots of edge dispersions against the non-Hermitian parameter γ. Each panel is obtained by computing the eigenfrequencies of a supercell with periodic boundary condition along x direction and 20 unit cells along y direction. The top and bottom edges are covered by perfect electric conductors. The eigenfrequencies f are in units of GHz and the color scale in each panel indicates the imaginary part of the eigenfrequencies.

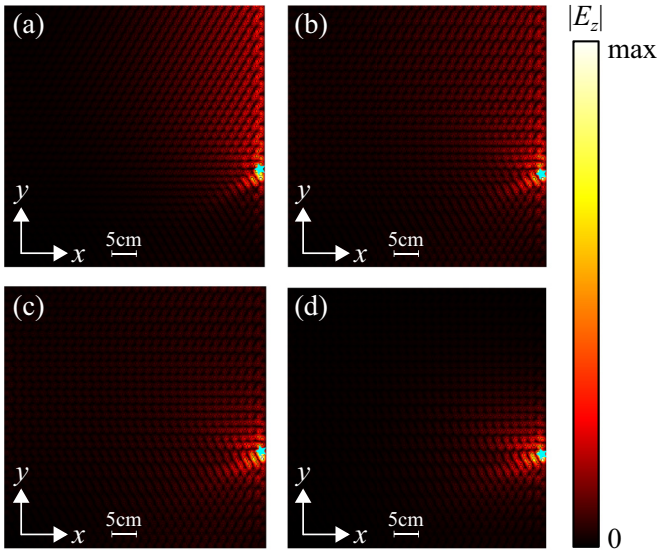

FIG. 4. Simulated out-of-plane electric field ($|E_z|$) distributions in finite photonic lattices with different values of γ. Panels (a) to (d) represent the field distributions with $\gamma = 0$, 2.2, 3.05, and 3.9, respectively. The cyan star in each panel denotes the point source operating at 4.68 GHz. The right boundary is chosen as a perfect electric conductor, while the three remaining boundaries are set as scattering boundaries. Chiral edge modes are observed at $\gamma = 0$ and 2.2 (topological phase), whereas electric field decays rapidly away from the source when $\gamma = 3.05$ (transition point) and 3.9 (trivial phase).

the yellow region in the band gap window). By inspecting the dispersions near the Dirac cone region [see Figs. 2(e)–2(h)], it can be observed that this process is accompanied by the closing and reopening of the Dirac cone. Notably, during the transition, the eigenfrequencies around the Dirac cone remain almost real (the imaginary part of the eigenfrequencies is negligibly small), while the complex spectra are only observed at frequencies far from the band gap. This in turn indicates that the band gap closing and reopening process is similar to those driven by Hermitian parameters in Hermitian systems.

In order to investigate whether the bulk band gap closing and reopening correspond to a topological phase transition, we compute the edge dispersions for the same set of γ. Specifically, we consider a supercell with periodic boundary condition along x direction and 20 unit cells along y direction. The top and bottom edges are covered by perfect electric conductors to avoid the leakage of the edge modes.

As shown in Fig. 3(a), the edge dispersion $\gamma = 0$ exhibits two purely real bands that span the band gap. These two bands are indeed the chiral edge modes that are localized at the top and bottom edges. When γ increases to 2.2 [see Fig. 3(b)], the spectrum looks similar to the Hermitian case, with the band gap of the bulk Dirac cone becoming smaller. Both of the chiral edge modes still remain, but they acquire nonzero imaginary eigenfrequencies due to the gain and loss at the edges. When $\gamma = 3.05$, as depicted in Fig. 3(c), the bulk spectrum becomes gapless, which is consistent with the band gap closing predicted by the bulk band diagrams [see Figs. 2(c) and 2(g)]. By further increasing γ to 3.9, the band gap opens again. In this case, however, there are no in-gap modes [see Fig. 3(c)], indicating this as a trivial insulator phase. Thus, by tuning the non-Hermitian parameter γ, we can indeed switch on or off the chiral edge modes and realize a topological phase transition.

To further visualize the topological phase transition above, we simulate the field distributions excited by a point source for the same set of γ as in Figs. 2 and 3. We consider a finite lattice comprised of 30×20 unit cells along x and y directions, respectively. The right boundary is covered by a perfect electric conductor, whereas the remaining boundaries are set to be scattering boundaries. A point source operating at 4.68 GHz (in the middle of the band gap) is placed at the right edge, as labeled as the cyan star in each panel of Fig. 4.

Before the topological phase transition takes place, the unidirectional propagation of the chiral edge modes is observed as shown in Figs. 4(a) and 4(b). At the transition point, the unidirectional propagation disappears and the fields are confined around the source due to the low density of states around the Dirac point frequency [see Fig. 4(c)]. When $\gamma = 3.9$, the source operates at the frequency in the trivial band gap where the density of states vanishes. Consequently, the excited fields become more confined to the source as illustrated in Fig. 4(d). These simulations again verify the existence of topological phase transition in the system when the non-Hermitian parameter γ is tuned.

It is noteworthy that, in the simulation above, the chiral edge modes are chosen to be excited at the armchair edge, i.e., the vertical edge for a clearer demonstration since the gain and loss are balanced along this edge. However, at other types of edges including the zigzag edge, the chiral edge

modes can be amplified or attenuated according to the local gain and loss profile at the specific edge. This gives rise to the possibilities of non-Hermitian control over the chiral edge modes in addition to mere switching on or off the chiral edge modes. Furthermore, when considering a finite lattice with all boundaries covered by perfect electric conductors, the amplifying and decaying chiral edge modes can lead to the non-Hermitian skin effect [49–51].

To conclude, we have realized a topological phase transition via on-site gain and loss in a photonic Chern insulator. The Hermitian limit of our design has been proven practically feasible in many previous microwave experiments [7,48,52]. The non-Hermitian components in our proposal can be implemented in a lossy medium with additional loss applied to certain sites, i.e., on-site gain is not necessary [25]. Towards higher frequencies, similar topological phase transition may be observed in laser-written optical waveguide systems, where tunable on-site loss can be realized through small breaks in the waveguides [53]. It is also possible for the proposed phenomenon to be realized in an active system where reconfigurable control of the chiral edge modes and topological lasing can be explored.

This work is supported by Singapore Ministry of Education Academic Research Fund Tier 3 under Grant No. MOE2016-T3-1-006.

[1] M. Z. Hasan and C. L. Kane, Colloquium: Topological insulators, Rev. Mod. Phys. **82**, 3045 (2010).
[2] X.-L. Qi and S.-C. Zhang, Topological insulators and superconductors, Rev. Mod. Phys. **83**, 1057 (2011).
[3] L. Lu, J. D. Joannopoulos, and M. Soljačić, Topological photonics, Nat. Photon. **8**, 821 (2014).
[4] A. B. Khanikaev and G. Shvets, Two-dimensional topological photonics, Nat. Photon. **11**, 763 (2017).
[5] T. Ozawa, H. M. Price, A. Amo, N. Goldman, M. Hafezi, L. Lu, M. C. Rechtsman, D. Schuster, J. Simon, O. Zilberberg, and I. Carusotto, Topological photonics, Rev. Mod. Phys. **91**, 015006 (2019).
[6] Z. Wang, Y. D. Chong, J. D. Joannopoulos, and M. Soljačić, Reflection-Free One-Way Edge Modes in a Gyromagnetic Photonic Crystal, Phys. Rev. Lett. **100**, 013905 (2008).
[7] Z. Wang, Y. Chong, J. D. Joannopoulos, and M. Soljačić, Observation of unidirectional backscattering-immune topological electromagnetic states, Nature (London) **461**, 772 (2009).
[8] M. Hafezi, E. A. Demler, M. D. Lukin, and J. M. Taylor, Robust optical delay lines with topological protection, Nat. Phys. **7**, 907 (2011).
[9] A. B. Khanikaev, S. Hossein Mousavi, W.-K. Tse, M. Kargarian, A. H. MacDonald, and G. Shvets, Photonic topological insulators, Nat. Mater. **12**, 233 (2013).
[10] M. Hafezi, S. Mittal, J. Fan, A. Migdall, and J. Taylor, Imaging topological edge states in silicon photonics, Nat. Photon. **7**, 1001 (2013).
[11] W.-J. Chen, S.-J. Jiang, X.-D. Chen, B. Zhu, L. Zhou, J.-W. Dong, and C. T. Chan, Experimental realization of photonic topological insulator in a uniaxial metacrystal waveguide, Nat. Commun. **5**, 5782 (2014).
[12] L.-H. Wu and X. Hu, Scheme for Achieving a Topological Photonic Crystal by Using Dielectric Material, Phys. Rev. Lett. **114**, 223901 (2015).
[13] T. Ma and G. Shvets, All-Si valley-Hall photonic topological insulator, New J. Phys. **18**, 025012 (2016).
[14] J.-W. Dong, X.-D. Chen, H. Zhu, Y. Wang, and X. Zhang, Valley photonic crystals for control of spin and topology, Nat. Mater. **16**, 298 (2017).
[15] F. Gao, H. Xue, Z. Yang, K. Lai, Y. Yu, X. Lin, Y. Chong, G. Shvets, and B. Zhang, Topologically protected refraction of robust kink states in valley photonic crystals, Nat. Phys. **14**, 140 (2018).
[16] Z. Gao, Z. Yang, F. Gao, H. Xue, Y. Yang, J. Dong, and B. Zhang, Valley surface-wave photonic crystal and its bulk/edge transport, Phys. Rev. B **96**, 201402(R) (2017).
[17] X. Wu, Y. Meng, J. Tian, Y. Huang, H. Xiang, D. Han, and W. Wen, Direct observation of valley-polarized topological edge states in designer surface plasmon crystals, Nat. Commun. **8**, 1304 (2017).
[18] M. C. Rechtsman, J. M. Zeuner, Y. Plotnik, Y. Lumer, D. Podolsky, F. Dreisow, S. Nolte, M. Segev, and A. Szameit, Photonic Floquet topological insulators, Nature (London) **496**, 196 (2013).
[19] F. Gao, Z. Gao, X. Shi, Z. Yang, X. Lin, H. Xu, J. D. Joannopoulos, M. Soljačić, H. Chen, L. Lu *et al.*, Probing topological protection using a designer surface plasmon structure, Nat. Commun. **7**, 11619 (2016).
[20] L. J. Maczewsky, J. M. Zeuner, S. Nolte, and A. Szameit, Observation of photonic anomalous Floquet topological insulators, Nat. Commun. **8**, 13756 (2017).
[21] S. Mukherjee, A. Spracklen, M. Valiente, E. Andersson, P. Öhberg, N. Goldman, and R. R. Thomson, Experimental observation of anomalous topological edge modes in a slowly driven photonic lattice, Nat. Commun. **8**, 13918 (2017).
[22] L. Lu, L. Fu, J. D. Joannopoulos, and M. Soljačić, Weyl points and line nodes in gyroid photonic crystals, Nat. Photon. **7**, 294 (2013).
[23] L. Lu, Z. Wang, D. Ye, L. Ran, L. Fu, J. D. Joannopoulos, and M. Soljačić, Experimental observation of Weyl points, Science **349**, 622 (2015).
[24] W.-J. Chen, M. Xiao, and C. T. Chan, Photonic crystals possessing multiple Weyl points and the experimental observation of robust surface states, Nat. Commun. **7**, 13038 (2016).
[25] C. Poli, M. Bellec, U. Kuhl, F. Mortessagne, and H. Schomerus, Selective enhancement of topologically induced interface states in a dielectric resonator chain, Nat. Commun. **6**, 6710 (2015).
[26] J. M. Zeuner, M. C. Rechtsman, Y. Plotnik, Y. Lumer, S. Nolte, M. S. Rudner, M. Segev, and A. Szameit, Observation of a Topological Transition in the Bulk of a Non-Hermitian System, Phys. Rev. Lett. **115**, 040402 (2015).
[27] S. Weimann, M. Kremer, Y. Plotnik, Y. Lumer, S. Nolte, K. G. Makris, M. Segev, M. C. Rechtsman, and A. Szameit, Topologically protected bound states in photonic parity–time-symmetric crystals, Nat. Mater. **16**, 433 (2017).

[28] L. Xiao, X. Zhan, Z. Bian, K. Wang, X. Zhang, X. Wang, J. Li, K. Mochizuki, D. Kim, N. Kawakami *et al.*, Observation of topological edge states in parity–time-symmetric quantum walks, Nat. Phys. **13**, 1117 (2017).

[29] L. Xiao, T. Deng, K. Wang, G. Zhu, Z. Wang, W. Yi, and P. Xue, Non-Hermitian bulk–boundary correspondence in quantum dynamics, Nat. Phys. **16**, 761 (2020).

[30] S. Weidemann, M. Kremer, T. Helbig, T. Hofmann, A. Stegmaier, M. Greiter, R. Thomale, and A. Szameit, Topological funneling of light, Science **368**, 311 (2020).

[31] K. Kawabata, K. Shiozaki, M. Ueda, and M. Sato, Symmetry and Topology in Non-Hermitian Physics, Phys. Rev. X **9**, 041015 (2019).

[32] H. Zhou and J. Y. Lee, Periodic Table for topological bands with non-Hermitian symmetries, Phys. Rev. B **99**, 235112 (2019).

[33] Z. Gong, Y. Ashida, K. Kawabata, K. Takasan, S. Higashikawa, and M. Ueda, Topological Phases of Non-Hermitian Systems, Phys. Rev. X **8**, 031079 (2018).

[34] M. A. Bandres, S. Wittek, G. Harari, M. Parto, J. Ren, M. Segev, D. N. Christodoulides, and M. Khajavikhan, Topological insulator laser: Experiments, Science **359**, eaar4005 (2018).

[35] K. Takata and M. Notomi, Photonic Topological Insulating Phase Induced Solely by Gain and Loss, Phys. Rev. Lett. **121**, 213902 (2018).

[36] X.-W. Luo and C. Zhang, Higher-Order Topological Corner States Induced by Gain and Loss, Phys. Rev. Lett. **123**, 073601 (2019).

[37] Y.-J. Wu, C.-C. Liu, and J. Hou, Wannier-type photonic higher-order topological corner states induced solely by gain and loss, Phys. Rev. A **101**, 043833 (2020).

[38] Y. Ao, X. Hu, Y. You, C. Lu, Y. Fu, X. Wang, and Q. Gong, Topological Phase Transition in the Non-Hermitian Coupled Resonator Array, Phys. Rev. Lett. **125**, 013902 (2020).

[39] K. Wang, A. Dutt, K. Y. Yang, C. C. Wojcik, J. Vučković, and S. Fan, Generating arbitrary topological windings of a non-Hermitian band, Science **371**, 1240 (2021).

[40] K. Kawabata, K. Shiozaki, and M. Ueda, Anomalous helical edge states in a non-Hermitian Chern insulator, Phys. Rev. B **98**, 165148 (2018).

[41] H. C. Wu, L. Jin, and Z. Song, Inversion symmetric non-Hermitian Chern insulator, Phys. Rev. B **100**, 155117 (2019).

[42] H. Xue, Q. Wang, B. Zhang, and Y. D. Chong, Non-Hermitian Dirac Cones, Phys. Rev. Lett. **124**, 236403 (2020).

[43] H. Shen, B. Zhen, and L. Fu, Topological Band Theory for Non-Hermitian Hamiltonians, Phys. Rev. Lett. **120**, 146402 (2018).

[44] A. Cerjan, M. Xiao, L. Yuan, and S. Fan, Effects of non-Hermitian perturbations on Weyl Hamiltonians with arbitrary topological charges, Phys. Rev. B **97**, 075128 (2018).

[45] F. D. M. Haldane, Model for a Quantum Hall Effect without Landau Levels: Condensed-Matter Realization of the "Parity Anomaly", Phys. Rev. Lett. **61**, 2015 (1988).

[46] D. Leykam, S. Mittal, M. Hafezi, and Y. D. Chong, Reconfigurable Topological Phases in Next-Nearest-Neighbor Coupled Resonator Lattices, Phys. Rev. Lett. **121**, 023901 (2018).

[47] S. Stützer, Y. Plotnik, Y. Lumer, P. Titum, N. H. Lindner, M. Segev, M. C. Rechtsman, and A. Szameit, Photonic topological Anderson insulators, Nature (London) **560**, 461 (2018).

[48] G.-G. Liu, P. Zhou, Y. Yang, H. Xue, X. Ren, X. Lin, H.-x. Sun, L. Bi, Y. Chong, and B. Zhang, Observation of an unpaired photonic Dirac point, Nat. Commun. **11**, 1873 (2020).

[49] V. M. Martinez Alvarez, J. E. Barrios Vargas, and L. E. F. Foa Torres, Non-Hermitian robust edge states in one dimension: Anomalous localization and eigenspace condensation at exceptional points, Phys. Rev. B **97**, 121401(R) (2018).

[50] Y. Xiong, Why does bulk boundary correspondence fail in some non-Hermitian topological models, J. Phys. Commun. **2**, 035043 (2018).

[51] S. Yao and Z. Wang, Edge States and Topological Invariants of Non-Hermitian Systems, Phys. Rev. Lett. **121**, 086803 (2018).

[52] Y. Poo, R. X. Wu, Z. Lin, Y. Yang, and C. T. Chan, Experimental Realization of Self-Guiding Unidirectional Electromagnetic Edge States, Phys. Rev. Lett. **106**, 093903 (2011).

[53] A. Cerjan, S. Huang, M. Wang, K. P. Chen, Y. Chong, and M. C. Rechtsman, Experimental realization of a Weyl exceptional ring, Nat. Photon. **13**, 623 (2019).